Biosensors and Bioelectronics 165 (2020) 112374

Contents lists available at ScienceDirect

Biosensors and Bioelectronics

journal homepage: http://www.elsevier.com/locate/bios

An impedance-coupled microfluidic device for single-cell analysis of primary cell wall regeneration

Lincai Chen [a,1], Ziyu Han [b,1], Xintong Fan [a], Shuaihua Zhang [b], Jiehua Wang [a,**], Xuexin Duan [b,*]

[a] School of Environmental Science and Engineering, Tianjin University, Tianjin, 300072, China
[b] State Key Laboratory of Precision Measuring Technology and Instruments, Tianjin University, Tianjin, 300072, China

ARTICLE INFO

Keywords:
Impedance spectroscopy
Microfluidics
Single plant cell
Primary cell wall (PCW) regeneration

ABSTRACT

Primary cell wall (PCW) is a rigid yet flexible cell wall surrounding plant cells and it plays key roles in plant growth, cell differentiation, intercellular communication, water movement and defence. As a technique widely used to study the characteristics of mammalian cells, electrical impedance spectroscopy (EIS) is rarely used in plant science. In this work, we designed and fabricated an EIS based biosensor coupled with microfluidic platform to investigate the formation process of PCWat the single-cell level. *Arabidopsis* mesophyll cells with completely regenerated PCW showed significantly higher impedance values compared to the nascent protoplasts without PCW, demonstrating that PCW formation caused a dramatic change in cell electrical properties. The device could also discriminate plant mutant cells with modified PCW compositions, thus provided a novel tool for physical phenotyping of plant cells. The dose-dependent effects of exogenously applied auxin on PCW regeneration were corroborated on this platform which revealed its potential to sensitively detect the influences of *in vitro* stimuli. This work not only provided one novel application of impedance-based biosensor to characterize a plant-specific developmental event, but also revealed the promises of EIS integrated microfluidic system as a sensitive, time-effective and low-cost platform to characterize single plant cells and make new scientific discoveries in plant science.

1. Introduction

Cells all have a cell membrane and plant cells go one step further to have a cell wall – an essential constituent that not only contributes to the success of plants colonizing the land by its complexity and recalcitrance, but also supplies our planet with many products such as food, wood and textiles. A full understanding of how plant cell wall is formed has been a hot-spot with vigorous research in the area of plant science and has continuously provided new insights into biotechnological innovations. In addition to providing mechanical supports (Bidhendi and Geitmann, 2016; De Lorenzo et al., 2019; Le Gall et al., 2015; Somerville et al., 2004), plant cell wall also plays key roles in plant growth, cell differentiation, intercellular communication, water transportation and defense against various stresses (Bidhendi and Geitmann, 2016; Le Gall et al., 2015). Two types of cell wall, namely primary cell wall (PCW) and secondary cell wall (SCW), exist in plants and they both consist of a network of interconnected polymers with diverse biochemical, mechanical and functional properties (Houston et al., 2016; Sakamoto et al., 2018). PCW is flexible to enable growth and is of sufficient mechanical strength to withstand the turgor pressure of the protoplast; while SCW is thick, inflexible and deposited between PCW and plasma membrane (PM) (Kumar et al., 2016; Zhang et al., 2018b). In this work, we focus on the *de novo* biosynthesis of PCW since it is chemically distinct, flexible, generally not lignified and more importantly, easier to deconstruct and faster to rebuild.

PCW consists of a network of rigid cellulose microfibrils (CMFs) embedded in a hydrated gel-like matrix containing non-cellulosic polysaccharides such as hemicellulose and pectin (Broxterman et al., 2018; Cosgrove, 2005; Novakovic et al., 2018; Tenhaken, 2014; Turner and Kumar 2018). The CMFs are synthesized by the cellulose synthase complexes (CSCs) located at plasma membrane (PM) and the matrix polysaccharides are produced in Golgi apparatus before being secreted into the wall for targeted deposition *via* vesicle transport (Oikawa et al., 2013). PCW is a complex structure that undergoes dynamic changes

* Corresponding author. author.
** Corresponding author. author.
E-mail addresses: jiehuawang@tju.edu.cn (J. Wang), xduan@tju.edu.cn (X. Duan).
[1] These authors contributed equally to this work.

https://doi.org/10.1016/j.bios.2020.112374
Received 28 January 2020; Received in revised form 29 May 2020; Accepted 7 June 2020
Available online 10 June 2020

during plant growth and development; however, it is hard to monitor the fate of one same cell along its full development (Sakai et al., 2019) through conventional methods due to the long culture period and low spatiotemporal resolution (Sanati Nezhad, 2014). The emergence of spectroscopy tools such as scanning electron microscope (SEM), transmission electron microscope (TEM) and atomic force microscope (AFM) (Braybrook, 2015; Cosgrove, 2018; Fromm et al., 2003; Gierlinger, 2018; Turner and Kumar 2018) have dramatically extended our understanding of the structural and biomechanical properties of PCW, whereas these visualization methods hardly provide complete and timely information of cell wall. Other easier, more direct and more convenient alternative biophysical tools are still highly desirable to understand the components and organization of PCW at single-cell level.

Based upon potentiometric, amperometric, or conductivity measurements, electrochemical sensors offer a wide range of applications including disease monitoring, drug discovery, environmental monitoring and food analysis. Electrochemical biosensors not only combine the electroanalytical sensitivity with its inherent biological selectivity but also are inexpensive, portable, and simple-to-operate compared to the conventional analytical tools (Karimi-Maleh et al., 2019; Ronkainen et al., 2010). Electrical impedance spectroscopy (EIS) has been widely used to measure the dielectric properties of cells and to assess cell status such as membrane permittivity and cytoplasmic conductivity (Tran et al., 2018; Zhang et al., 2018a; Zheng et al., 2013). One of the major advantages of EIS is that it is free of label or biochemical markers (Song et al., 2013) and identifies cell properties in a non-invasive manner (Li et al., 2018; Xu et al., 2016). Moreover, it is easy-to-use and flexible for design and fabrication. In recent years, benefiting from the integration with microfluidic techniques (Gawad et al., 2000; Giaever and Keese, 1984; K'Owino and Sadik, 2005; Liu et al., 2020; Tsai and Wang, 2016; Xu et al., 2016), EIS has been extensively applied in the field of cell biology, cancer research, drug screening and environmental safety monitoring. Nevertheless, such a technological advance has been primarily applied to animal and microbial cells, and very limited work has been conducted on plant cells so far (Jiang et al., 2014; Libault et al., 2017). In this study, we incorporated the microfluidic platform with microelectrodes to implement single-cell electrical impedance spectroscopy analysis on *Arabidopsis* mesophyll protoplast to characterize the plant-specific PCW regeneration process. The proposed microfluidic EIS device was fabricated not only to efficiently trap individual plant cells, but also to accurately monitor one unique biological program of plants without label and invasion. Our results demonstrated the capacity of such a device to differentiate plant mutant cells with varied PCW properties from their wild-type counterparts, thus providing a new phenotyping tool for single plant cells. Moreover, the varied cell electrical properties induced by auxin, one vital plant phytohormone, during PCW regeneration were investigated using the proposed method. By demonstrating the competence of this device to perform quantitative analysis on PCW reconstruction on the level of single cells, we envisioned the promises of EIS, when integrated with microfluidic, to offer versatile platforms for collecting novel biological information of distinct plant cells and help us gain new insights into complex plant biological phenomena at an unprecedented level of details.

2. Materials and methods

2.1. Design of the impedance-coupled microfluidic device for single plant cell analysis

The impedance-based microfluidic device is comprised of a polydimethylsiloxane (PDMS) layer which contains microfluidic channels for single plant cell trapping and three coplanar microelectrodes which are patterned on the bottom glass substrate for the purpose of applying electrical field and measuring differential current signals. Fig. 1A is a schematic diagram of the microfluidic channels for single-cell trapping, which is accomplished based on the hydrodynamic trapping mechanism (Tan and Takeuchi, 2007, 2008). Basically, the microfluidic channel is divided into two paths. Path 1 refers to the single cell trap, which contains two symmetrical semicircular structures with a radius of 30 μm (appropriately equivalent to the plant cell size as ~30–50 μm) and connected by a narrow channel with a width of 20 μm. Path 2 refers to a bypass channel with a width of 80 μm and is designed to have a higher flow resistance than Path 1. Under hydrostatic force, a cell is more likely to flow into Path 1 when the trap is empty. Once a cell is trapped at the semicircular trap, Path 1 will be blocked, and immediately exhibits a higher flow resistance than Path 2, in which case the following cells will flow into Path 2 and bypass the trapping cell. The height of the microfluidic channel is 70 μm to ensure a high trapping efficiency.

For impedance measurement, three parallel microelectrodes with width of 20 μm are located by 60 μm spacing underneath the trapping zone. The middle electrode is at the center of the two semicircular trapping structures and acts as an excitation electrode. The differential impedance measurement is conducted between the side two electrodes to eliminate the interference or noise caused by unexpected disturbances in the aquatic environment such as the changes in temperature and pH (Gawad et al., 2004).

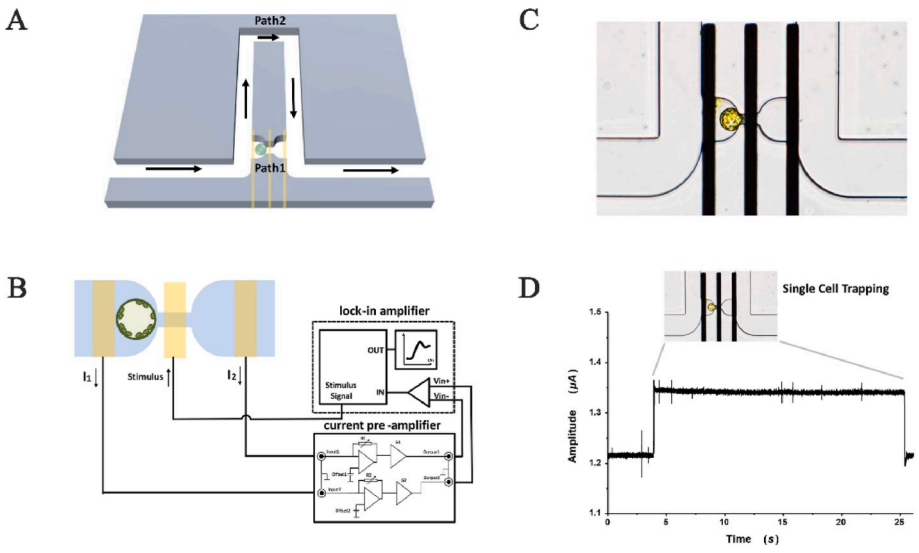

Fig. 1. Microfluidic impedance spectroscopy platform for monitoring single plant cells. (A) Schematic diagram of the microfluidic chip for single plant cell trapping. The microfluidic channel was divided into two paths, Path 1 and Path 2. Three parallel impedance sensing microelectrodes (yellow color) were located underneath the trapping zone. (B) Schematic diagram of the impedance sensing setup. The middle electrode was patterned at the center of the two semicircular trapping structures and acted as an excitation electrode. (C) Microscope image of a trapped *Arabidopsis* mesophyll cell. Flow direction was from left to right. (D) Real-time current response of a captured cell showing that once a cell was trapped in the sensing trap, the current signal was increased. . (For interpretation of the references to color in this figure legend, the reader is referred to the Web version of this article.)

2.2. Experimental procedure for impedance measurement of single plant cell

The detailed experimental procedure for impedance measurement of single plant cell is described in Supplementary Information. In brief, after a calibration process performed before each test, the cell suspension is continuously pumped into the microfluidic chip by a pressure-driven pump (Fluidgent MFCS EZ, France) under a constant driven pressure of 10 mbar. An impedance analyzer (Zurich Instruments HF2IS, Switzerland) is employed to apply the excitation electric signal (1 V, ranging from 1 kHz to 10 MHz, with 30 points per decade of frequency) on the middle electrode. The differential current responses on the side two electrodes are pre-amplified by 1000 A/V through a current pre-amplifier (Zurich Instruments HF2TA, Switzerland) and recorded by the impedance analyzer. The imaginary component of the differential current versus frequency is extracted to elucidate the change on membrane compositions during PCW regeneration. The acquired data are processed and analyzed by a Matlab program and plotted by Origin. An inverted fluorescence microscope (Olympus IX53, Japan) attached with a CCD camera (Olympus DP73, Japan) is used to observe the microfluidic device and capture cell images.

2.3. Microfluidic device fabrication

The microelectrodes, comprised by 50 nm Ti and 200 nm Au, are patterned on the BF33 glass substrate by a conventional lift-off process. The master molds of the microfluidic channels are fabricated by a standard photolithography process using the negative photoresist SU-8 (Micro Chem). The microfluidic channels are fabricated by a conventional soft-lithography technique using PDMS (Mcdonald and Whitesides, 2002; Ng et al., 2002) (Dowcorning Sylgard 184). In brief, the PDMS base and the curing agent are mixed at a ratio of 10 (base):1 (curing agent). The well mixed PDMS is poured on the master mold and vacuumed to further eliminate the bubbles generated during mixing. The master mold together with uncured PDMS is then baked under 95 °C for 30 min to cure the PDMS film. After peeled off from the master mold, the PDMS film is cut into individual PDMS chip and punched for liquid inlets and outlets. The PDMS chip and glass substrate are aligned and irreversibly bonded after an oxygen plasma treatment. The fabricated device is then attached to a PCB board, and the connection with external instruments is achieved by wire bonding the microelectrodes to the gold pads on PCB board and plugging the PCB board into a self-designed connector.

2.4. Arabidopsis protoplast isolation and PCW regeneration

All plants used in this study are *Arabidopsis thaliana* in Columbia-0 (Col-0) ecotype background. The *rsw1-1* (CS6554), *prc1-1* (CS297) and *polygalacturonase* (CS859528) mutants are obtained from the Arabidopsis Biological Resource Center (http://abrc.osu.edu). Plants are grown in a greenhouse with a cycle of 16 h light/8 h dark under fluorescent white light at 20 °C.

Arabidopsis mesophyll protoplasts are isolated according to the method previously reported with minor modification (see Supplementary Information) (Yoo et al., 2007). In brief, the healthy and fully expanded *Arabidopsis* leaves (3-4-week-old, as shown in Fig. S1) are washed, sliced into fine strips (0.5–1.0 mm) and immediately transferred into the freshly made enzyme solution (1.5% cellulase R10, 0.4% macerozyme R10, 0.4 M mannitol, 20 mM KCl, 10 mM MES at pH 5.8). The reaction is heated for 10 min at 55 °C and cooled down to room temperature before adding 10 mM $CaCl_2$ and 0.1% BSA and being incubated in darkness at 26 °C for at least 3 h. After the enzymatic digestion, the enzymatic digestion is stopped by an equal volume of W5 solution (154 mM NaCl, 125 mM $CaCl_2$, 5 mM KCl, 2 mM MES at pH 5.8). Protoplasts are obtained by filtering the solution through a 75 μm nylon mesh into 50 ml round-bottom tubes with 20 ml W5 solution. After centrifugation at 100*g* for 6 min, the pellet is re-suspended in culture medium (0.32% B-5 medium, 0.25 M mannitol, 4 mM MES at pH 5.8, see Supplementary Information) by gentle swirling. Then the solution is centrifuged at 100 g for 6 min again and after decanting the supernatant, protoplasts are re-suspended in culture medium at a concentration of approximately 10^5 cells/ml as determined by a hemocytometer. Next, the protoplasts are transferred into 24-well culture plates and incubated in the dark at room temperature for further analysis. In exogenous auxin stimulation experiments, the protoplasts are incubated together with 5, 50 and 250 μM 1-naphthylacetic acid (NAA). The viability of cells is determined using the fluorescein diacetate (FDA) staining method (Larkin, 1976) and the regenerated primary cell wall of protoplasts is stained with fluorescent brightener, Calcofluor white (Nagata and Takebe, 1970). All chemicals are obtained from Sigma-Aldrich, except for Cellulase R10 and Macerozyme R10, which are purchased from Yakult Pharmaceutical Ind. Co., Ltd. (Japan).

2.5. Scanning electron microscopic observation

Cells are fixed with 2.5% glutaraldehyde (pH 6.0) at 4 °C for 2 h, and washed with 0.4 M mannitol before replaced with 30%, 50%, 70%, 80%, 90%, 100% ethanol solutions for 15 min. They are dehydrated twice with 100% ethanol, and placed on a slide glass whose surface is pre-treated with poly-L-tyrosine to lyophilize the cells with vacuum freeze-drying equipment. The specimens are slightly coated with 9 nm layer of gold by an ion spatter coater, and the coated-specimens were observed with a scanning electron microscope (Inspect F50, Thermo Fisher Scientific, USA) at 20 kV.

3. Results and discussion

3.1. Single plant cell trapping and monitoring on a microfluidic device

In order to perform impedance measurements on single plant cells, a suspension of *Arabidopsis* mesophyll protoplasts at an approximate concentration of 1×10^5 cells/ml was introduced into the microfluidic channel. The fluid flow direction was from left to right driven by a pressure pump and a single plant cell was captured in the left trap (e.g. the sensing trap) with the right trap facing to the left remaining empty (e.g. the reference trap) (Fig. 1A). The excitation electric signal was applied on the middle electrode while the differential current responses on the side two electrodes are pre-amplified by 1000 A/V and measured by the impedance analyzer (Fig. 1B). After being successfully captured in the sensing trap with an empty reference trap (Fig. 1C), a single plant cell was measured for its real-time differential current (Fig. 1D). Notably, different from animal cells, plant cells are structurally fragile without the protection of cell wall and some spikes were observed in the differential current curve, which was likely caused by the cellular debris from cell lysis during cell preparation process. In order to avoid such background noises, the protoplast preparation procedure needed to be optimized to obtain uniform and synchronous plant cells and an isotonic environment should be provided to ensure the cell integrity. During the impedance measurements, the driven pressure was decreased to 2 mbar to minimize the fluid shear stress-induced cell rupture. Besides, similar results should be obtained from two sets of devices with adequate biological and experimental replications. To summarize, as shown by a previous study focusing on the differentiation process of mouse embryonic stem cell (mESC) using electrical impedance measurements on a similar microfluidic device (Zhou et al., 2016), our work demonstrated that plant cells could also be efficiently captured for concomitant electrical impedance measurements at single cell level.

3.2. Electrical equivalent model for plant cell wall formation

In this work, plant cell is defined as a single shell model (Morgan et al., 2007; Sun et al., 2008) (Supplementary Information), which is

composed of a conducting sphere of cytoplasm and an insulating thin shell (cell membrane plus cell wall) (see Fig. S2A in Supplementary Information). Composed of species-specific amounts of various proteins and a double layer of lipids, the single shell is as thin as 5–10 nm and isolates the cytoplasm from the ambient medium. Fig. 2A shows an ideal electrical equivalent model representing a plant cell suspended in the culture medium in the single-cell trapping device. The total complex impedance of a suspended plant cell and that of the medium in the reference trap are referred as Z_{mix} and Z_{med}, respectively. When taking into consideration the electrical double layer capacitance (C_{dl}) between the coplanar electrode surface and the medium electrolyte, the overall impedance measured between the excitation electrode and the sensing electrodes are referred as Z_{sense} and Z_{ref}, respectively. The measured currents and the differential impedance could thus be obtained by subtracting the I_{ref} and Z_{ref} from the I_{sense} and Z_{sense}, respectively (Malleo et al., 2010) and the derivation of Z_{sense} and Z_{ref} from I_{sense} and I_{ref} is described in Supplementary Information.

Since PCW is a regenerated structure closely attaching to the original cell membrane, the changes in the dielectric property of the newly formed cell "coat" composed of plasma membrane plus PCW are analyzed in this study using the single shell model. As shown in Fig. 2B, after PCW regeneration, the total membrane capacitance ($C_{mem+wall}$) is presumed to be different from that of original protoplast (C_{mem}) due to their divergent compositions and thickness, which is mainly related to the changes in the imaginary part of the measured currents (see the derivation of electrical equivalent model in the Supplementary Information). Thus, we used the imaginary parts of the differential current and impedance to characterize the changes in the dielectric property of cell membrane caused by PCW regeneration in the following analysis. Meanwhile, considering that the total impedance was dominant by the electrical double layer capacitance in the low frequency range ($f < 100$ kHz) and the cytoplasm properties could be characterized at the high frequency range ($f > 10$ MHz) (McGrath et al., 2017), we narrowed down the frequency range to 100 kHz to 2 MHz in order to focus on the impedance changes induced by the membrane composition and to eliminate the influence of the double layer capacitance.

3.3. EIS characterization of single plant cell at different PCW wall regeneration status

In order to test the possibility of using EIS to characterize PCW, we prepared *Arabidopsis* mesophyll cells at three status of cell wall status, including protoplasts without PCW (after 0 h incubation), cells at transition phase (after 12 h incubation), and cells with fully regenerated PCW (after 24 h incubation). At each phase, cells upon impedance measurement were concomitantly stained with a fluorescent brightener which conjugates with cellulose within PCW and emits blue light under the excitation of ultraviolet light, to verify the correlation between the newly regenerated PCW structure and the impedance parameters of plant cells. Besides, SEM was applied to directly visualize the microstructure of newly formed PCW. Fresh protoplasts released from leaves were spherical and appeared transparent with chloroplasts lying beneath the plasmalemma (Fig. 3A–a), and florescent staining confirmed that the smooth surface of these cells was devoid of cell wall components (Fig. 3B–a). In contrast, after 12 h of incubation, some faint fibrillar network imprints with random distribution appeared on the membrane surface (Fig. 3A-b) accompanied with a faint but detectable blue signal in the fluorescence image (Fig. 3B–b), implicative of the deposition of cellulose at this time-point. After 24 h, the whole cell was covered with the fibrillar network and the membrane became invisible (Fig. 3A–c). With the fibrillar network getting thick and convoluted, a strong fluorescence signal gradually emerged (Fig. 3B-c) with finer structures appearing as fibrils embedded within the surface, which could be due to the removal of amorphous components during the fixation and dehydration procedures (Burgess and Linstead, 1976). Thus, optical characterizations confirmed distinct morphological properties and microstructures of cells at different PCW regeneration status, and validated the potential of using EIS to directly detect the formation of primary cell wall. The EIS measurements of single cells at different PCW regeneration status were shown in Fig. 3C–E. In a given frequency range from 1 kHz to 10 MHz, 100 kHz to 2 MHz yielded the highest sensitivity in discriminating cells at different PCW phases as judged by the imaginary part of impedance spectra (Fig. 3F). This result was in agreement with the previously published work suggesting that the maximum difference occurred around 1 MHz for the changes in cell membrane capacitance (Gawad et al., 2004). In this work, when the electrical excitation frequency was set in the range from 100 kHz to 2 MHz for a better resolution, the impedance imaginary parts of highest magnitude were observed for 24 h cells with fully regenerated PCW when compared to protoplasts and cells at 12 h. This result was consistent with SEM results that the entire surface of protoplasts was covered with a thick and convoluted network of PCW materials after 24 h of regeneration, which resulted in decreased capacitance of cell membrane and PCW, and in turn increased the impedance imaginary parts of cells. Notably, individual cells in the same population exhibited fluctuations in their impedance responses, which was likely due to the various extents of their PCW regeneration and the heterogeneity in other characteristics such as cell shape and the final cell location during the trapping process (Zhou et al., 2016). Despite of this, the averaged impedance spectra still represented the typical impedance response of a particular cell population, and the increment in the imaginary part of the overall impedance of cells from 0 h to 24 h implied the dramatic changes in their membrane capacitance (Fig. 3F). Taken together, the results described above demonstrated that the proposed device could recognize the behavior of single plant cell and efficiently monitor PCW regeneration process at optimized frequencies in a real-time manner, which holds the promise to be extended to monitor other complex biological activities of plant cells.

3.4. Impedance measurement of PCW regeneration of mutant cells

One of the most interesting studies of plant cells is to understand PCW biosynthesis and its regulation at the molecular level. As an integral part of plant genetics, the study of mutants has enormously progressed gene functional analysis by establishing a connection between

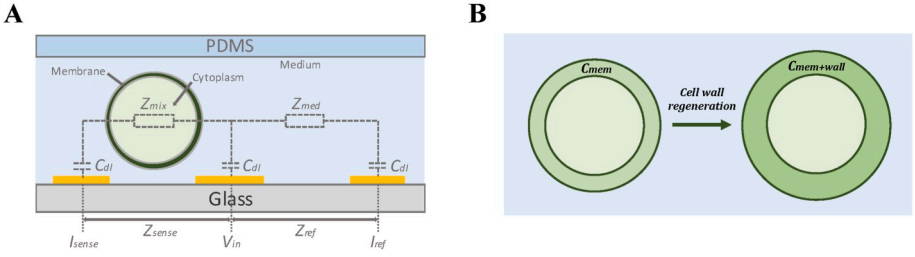

Fig. 2. Electrical equivalent model of a plant cell inside the microfluidic impedance system. (A) An ideal electrical equivalent model representing a plant cell suspended in the culture medium in the trapping device. (B) Schematic diagram illustrating the change of the equivalent models before and after the regeneration of plant primary cell wall.

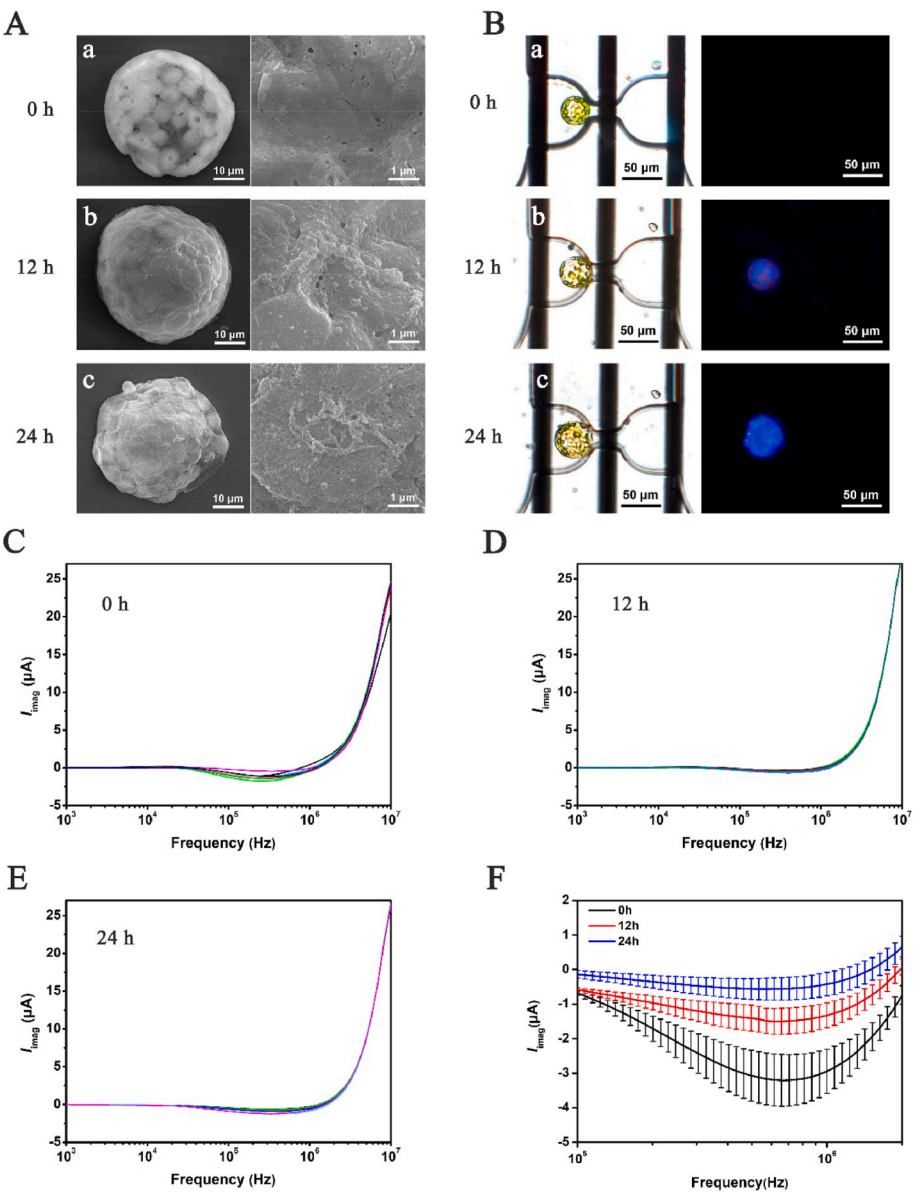

Fig. 3. Impedance spectrums of single plant cells at different status of primary cell wall regeneration. (A) Scanning electron micrographs of cells following 0 h, 12 h and 24 h of regeneration, in each figure, high magnification of the whole cell is shown on the right. (B) *In situ* fluorescence images of PCW (blue) for single plant cells at different time-points (0 h, 12 h and 24 h), respectively. (C) (D)and (E) The imaginary part of impedance for single plant cells at different status (0 h, 12 h and 24 h), respectively. (F) The average imaginary part of impedance of (C) (D) and (E). Each experimental data point shows the average value of ten cells. Error bars show the standard deviation. . (For interpretation of the references to color in this figure legend, the reader is referred to the Web version of this article.)

the absence of specific gene in an organismal or cellular context and the resultant phenotypic changes. For conventional transgenic approach, plants are usually grown for a long time before gene functions to be analyzed at the level of entire plant, organ, or tissue, in which case transitory phenotypes have a big chance to be masked by the cellular complexity of the analyzed sample and the functional redundancy of gene family members.

As mentioned above, the impedance measurement could monitor the PCW regeneration status of individual plant cells and thus potentially provide a convenient tool to test cell mutant with different PCW composition. We then used the proposed device to characterize cells from several *Arabidopsis thaliana* mutant lines that are defective in genes related to PCW composition. As the most abundant and useful biopolymer on the earth and the major component of PCW, cellulose is a crystalline polysaccharide providing mechanical strength which is central to plant morphogenesis. Cellulose is synthesized by structures embedded in the plasma membrane known as cellulose synthase (CesA) complexes (CSC) or particle rosettes before being secreted (McFarlane et al., 2014). In this work, *rsw1-1* and *prc1-1* mutants defective in *CesA1* and *CesA6*, respectively; were used since that both mutated genes are required to deposit cellulose in PCW (Arioli et al., 1998; Fagard et al., 2000). Possessing fewer rosettes than WT plants, *rsw1-1* mutant shows temperature-sensitive reduction in its cellulose synthesis and accumulates non-crystalline β-1, 4-glucan (Arioli et al., 1998; Turner and Kumar 2018). The *prc1-1* mutation causes a structural deregulation in PCW of growing cells and is also impaired in the production of cellulose as *rsw1-1* (Fagard et al., 2000). We also included another mutant defective in polygalacturonase, which is involved in hydrolyzing pectic polysaccharides within PCW and the middle lamellae (Alonso et al., 2003; Caffall and Mohnen, 2009), instead of being directly involved in the biosynthesis of PCW.

Three types of *Arabidopsis* mutant cells were then analyzed for their respective impedance responses during PCW regeneration process at a frequency range set from 100 kHz to 2 MHz in parallel with the wild-type (WT) cells. As shown in Fig. 4, at the nascent protoplast stage, three types of mutant cells showed similar impedance values as WT cells (Fig. 4A). After 12 h, WT and *polygalacturonase* mutant cells showed relatively higher impedance magnitudes than those of *rsw1-1* and *prc1-1* mutants (Fig. 4B), demonstrating that the defects in cellulose biosynthesis of the latter two mutants retarded the progress of PCW formation, changed the ultrastructure of their respective PCWs and resulted in decreased impedance values at the 12 h time-point. However, at 24 h

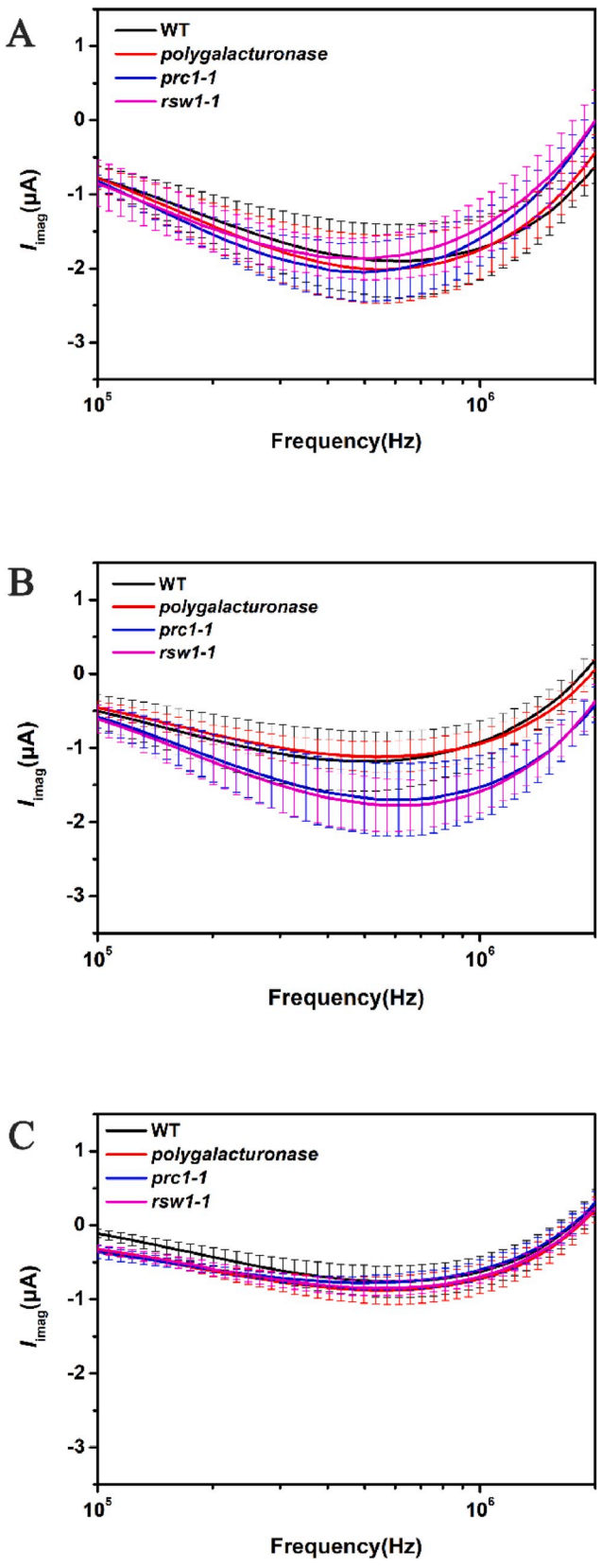

Fig. 4. Impedance spectrums of wild-type, *rsw1-1*, *prc1-1* and *polygalacturonase* mutants of *Arabidopsis thaliana* cells at frequency ranging from 100 kHz to 2 MHz. (A) (B) and (C) showing the average imaginary part of impedance for four cell types at different PCW regeneration status (0 h, 12 h and 24 h). Each experimental data point shows the average value of ten cells. Error bars show the standard deviation.

(Fig. 4C), the impedance spectra of four cell types reached similar values, indicating that at this stage, PCW regeneration of all cell types have been accomplished and no more significant variation in their impedance characters could be detected. Thus, it appeared that *rsw1-1* and *prc1-1* mutant cells were only negatively affected in cellulose scaffold assembling at the early stage of PCW regeneration, and such a temporary delay did not cause a final difference in their cellular electrical properties when compared to *polygalacturonase* mutant and WT cells. This explanation agrees with the previously published results that both mutants only display visible phenotypic abnormalities under limiting growth conditions (*rsw1-1* cells at stimulated metabolic rate when grown at 31 °C (Arioli et al., 1998)), or in specific organs undergoing rapid cell expansion (*rsw1-1* cells in expanding root cells during mitosis (Arioli et al., 1998) and *prc1-1* cells during hypocotyl cell expansion (Fagard et al., 2000)). Under these circumstances, fast cellulose synthesis and correct cellulose microfibril alignment are highly desirable (Sugimoto et al., 2001) to counteract the thinning of existing walls, which occurs as cells expand (Cosgrove, 1997), and to deposit cellulose in the new walls of dividing cells (Samuels et al., 1995). Such a rate demand for cellulose biosynthesis probably also occurs at the early stage of PCW regeneration, while at the later phase, the normal functions of the mutated genes could somehow be fulfilled or compensated, either through the deaccelerated local rates of cell wall synthesis or through the redundant functions of other gene family members. Previously, the complementary roles in PCW biosynthesis among *CesA* family members have been demonstrated for *CesA2*, *CesA5*, *CesA6* and *CesA9* (Griffiths et al., 2015; McFarlane et al., 2014).

To summarize, these results proved that the proposed impedance methodology enables a rapid and sensitive characterization of transient and subtle morphological abnormalities at single-cell level, which is difficult to be achieved in intact plants. Particularly, it has a high potential for early phenotyping screen of transgenic cells and could be employed as a complement to traditional plant approaches to obtain a more comprehensive view of gene functions.

3.5. Impedance measurement of in situ effects of auxin on PCW formation

Associations between hormone signaling and cell wall biosynthesis have long been suggested; however, the majority of relevant studies during recent decades have supported the hormone actions on cell wall architecture through indirect means. As a critical player involved in almost all aspects of plant growth and development, auxin performs a prominent regulatory role in cell wall architecture, particularly in cell wall loosening and cell expansion (Mockaitis and Estelle, 2008). Considering that the effects of auxin on PCW formation have not been effectively investigated at single-cell level, we analyzed the impedance responses of cells undergoing PCW regeneration upon auxin stimulation.

The effect of auxin on cell growth has been reported to be dose-dependent, with low and high doses eliciting distinct responses (Teale et al., 2006). Fig. 5 shows the effect of NAA (1-Naphthaleneacetic acid), a synthetic auxin derivative at concentrations of 5, 50 and 250 μM on cell impedance spectrum during PCW regeneration. Compared with the control group after 24 h, addition of 5 or 50 μM NAA had positive impacts on cell impedance responses indicating that these two concentrations of NAA significantly promoted the synthesis of PCW. In contrast, cells treated by NAA at 250 μM negatively influenced PCW regeneration and resulted in diminished impedance responses (Fig. 5). Such dose-dependent effects of auxin on cell impedance were consistent with a previous work using labeled glucose to detect the isotope incorporation into matrix polysaccharide synthesis (Baker and Ray, 1965), in which the authors demonstrated that a definite promotion of cell wall synthesis was induced by auxin at a concentration as low as 0.16 μM and the largest promotion of synthesis occurred at 1.6 and 16 μM IAA; however, at concentrations higher than 161 μM, a strong inhibition of cell wall synthesis was manifested (Baker and Ray, 1965). Thus, taken auxin as an example, our results confirmed the potential capacities of the

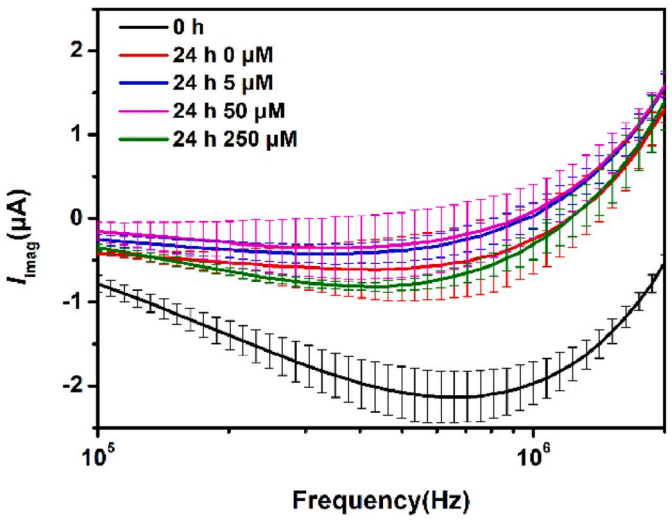

Fig. 5. Impedance spectra of *Arabidopsis thaliana* wild-type cells stimulated by three concentrations of 1-Naphthaleneacetic acid (NAA). Measured frequency in a range between 100 kHz and 2 MHz. Each experimental data point shows the average value of ten cells. Error bars show the standard deviation.

proposed platform to study plant cell responses to a variety of chemical and biological stimuli such as ions, salts, macromolecules as well as external cues to reveal the regulatory mechanisms associated with the plant cell system.

4. Conclusions

By integrating micro-scale electrodes with structured microfluidic channels, this study designed a non-invasive impedance platform to quantitatively assess single plant cell status during PCW regeneration, a process involving complex assembly and deposition of a variety of cellular components. By capturing single plant cells and simultaneously monitor the variations in their impedance parameters, the impedance device provides a powerful tool for botanists to understand this plant-unique phenomenon. This system also demonstrated its capability to discriminate wild-type cells from mutant cells with modified PCW properties and to corroborate the dose-dependency of auxin effects on PCW regeneration process at single-cell level. Taken together, this study laid a foundation for the development of more powerful biosensors to understand plant cell wall biosynthesis and its regulation at single-cell level. By providing highly precise and rapidly accessible cell/reagent handling capabilities, the impedance spectrum also envisioned high-throughput systems in a fully automated fashion and might be extended to plant cell cultivation, phenotypic screening, highly efficient cell transformation and gene expression at the single-cell resolution.

Declaration of competing interest

The authors declare that they have no known competing financial interests or personal relationships that could have appeared to influence the work reported in this paper.

CRediT authorship contribution statement

Lincai Chen: Conceptualization, Methodology, Visualization, Writing - original draft. **Ziyu Han:** Conceptualization, Methodology, Software, Writing - original draft. **Xintong Fan:** Investigation. **Shuaihua Zhang:** Investigation. **Jiehua Wang:** Supervision, Writing - review & editing. **Xuexin Duan:** Supervision, Writing - review & editing.

Acknowledgements

The authors gratefully acknowledge financial support from the National Key Research & Development Program of China (2016YFD0600103 and 2017YFF0204604), the National Natural Science Foundation of China (31870572, 61674114, 91743110, 21861132001), the Tianjin Applied Basic Research and Advanced Technology (17JCJQJC43600), the Foundation for Talent Scientists of Nanchang Institute for Microtechnology of Tianjin University, and the 111 Project (B07014).

Appendix A. Supplementary data

Supplementary data to this article can be found online at https://doi.org/10.1016/j.bios.2020.112374.

References

Alonso, J.M., Stepanova, A.N., Leisse, T.J., Kim, C.J., Chen, H.M., Shinn, P., Stevenson, D.K., Zimmerman, J., Barajas, P., Cheuk, R., Gadrinab, C., Heller, C., Jeske, A., Koesema, E., Meyers, C.C., Parker, H., Prednis, L., Ansari, Y., Choy, N., Deen, H., Geralt, M., Hazari, N., Hom, E., Karnes, M., Mulholland, C., Ndubaku, R., Schmidt, I., Guzman, P., Aguilar-Henonin, L., Schmid, M., Weigel, D., Carter, D.E., Marchand, T., Risseeuw, E., Brogden, D., Zeko, A., Crosby, W.L., Berry, C.C., Ecker, J.R., 2003. Genome-wide insertional mutagenesis of Arabidopsis thaliana. Science 301 (5633), 653–657.
Arioli, T., Peng, L., Betzner, A.S., Burn, J., Wittke, W., Herth, W., Camilleri, C., Hofte, H., Plazinski, J., Birch, R., Cork, A., Glover, J., Redmond, J., Williamson, R.E., 1998. Molecular analysis of cellulose biosynthesis in Arabidopsis. Science 279 (5351), 717–720.
Baker, D.B., Ray, P.M., 1965. Relation between effects of auxin on cell wall synthesis and cell elongation. Plant Physiol. 40 (2), 360–368.
Bidhendi, A.J., Geitmann, A., 2016. Relating the mechanics of the primary plant cell wall to morphogenesis. J. Exp. Bot. 67 (2), 449–461.
Braybrook, S.A., 2015. Measuring the elasticity of plant cells with atomic force microscopy. Methods Cell Biol. 125, 237–254.
Broxterman, S.E., van Erven, G., Schols, H.A., 2018. The solubility of primary plant cell wall polysaccharides in LiCl-DMSO. Carbohydr. Polym. 200, 332–340.
Burgess, J., Linstead, P.J., 1976. Scanning electron microscopy of cell wall formation around isolated plant protoplasts. Planta 131 (2), 173–178.
Caffall, K.H., Mohnen, D., 2009. The structure, function, and biosynthesis of plant cell wall pectic polysaccharides. Carbohydr. Res. 344 (14), 1879–1900.
Cosgrove, D.J., 1997. Assembly and enlargement of the primary cell wall in plants. Annu. Rev. Cell Dev. Biol. 13, 171–201.
Cosgrove, D.J., 2005. Growth of the plant cell wall. Nat. Rev. Mol. Cell Biol. 6 (11), 850–861.
Cosgrove, D.J., 2018. Diffuse growth of plant cell walls. Plant Physiol. 176 (1), 16–27.
De Lorenzo, G., Ferrari, S., Giovannoni, M., Mattei, B., Cervone, F., 2019. Cell wall traits that influence plant development, immunity, and bioconversion. Plant J. 97 (1), 134–147.
Fagard, M., Desnos, T., Desprez, T., Goubet, F., Refregier, G., Mouille, G., McCann, M., Rayon, C., Vernhettes, S., Hofte, H., 2000. PROCUSTE1 encodes a cellulose synthase required for normal cell elongation specifically in roots and dark-grown hypocotyls of Arabidopsis. Plant Cell 12 (12), 2409–2424.
Fromm, J., Rockel, B., Lautner, S., Windeisen, E., Wanner, G., 2003. Lignin distribution in wood cell walls determined by TEM and backscattered SEM techniques. J. Struct. Biol. 143 (1), 77–84.
Gawad, S., Cheung, K., Seger, U., Bertsch, A., Renaud, P., 2004. Dielectric spectroscopy in a micromachined flow cytometer: theoretical and practical considerations. Lab Chip 4 (3), 241–251.
Gawad, S., Heuschkel, M., Leung-Ki, Y., Iuzzolino, R., Schild, L., Lerch, P., Renaud, P., 2000. Fabrication of a microfluidic cell analyzer in a microchannel using impedance spectroscopy. In: 1st Annual International Ieee-Embs Special Topic Conference on Microtechnologies in Medicine & Biology, Proceedings, pp. 297–301.
Giaever, I., Keese, C.R., 1984. Monitoring fibroblast behavior in tissue culture with an applied electric field. Proc. Natl. Acad. Sci. U. S. A. 81 (12), 3761–3764.
Gierlinger, N., 2018. New insights into plant cell walls by vibrational microspectroscopy. Appl. Spectrosc. Rev. 53 (7), 517–551.
Griffiths, J.S., Sola, K., Kushwaha, R., Lam, P., Tateno, M., Young, R., Voiniciuc, C., Dean, G., Mansfield, S.D., DeBolt, S., Haughn, G.W., 2015. Unidirectional movement of cellulose synthase complexes in Arabidopsis seed coat epidermal cells deposit cellulose involved in mucilage extrusion, adherence, and Ray formation. Plant Physiol. 168 (2), 502–520.
Houston, K., Tucker, M.R., Chowdhury, J., Shirley, N., Little, A., 2016. The plant cell wall: a complex and dynamic structure as revealed by the responses of genes under stress conditions. Front. Plant Sci. 7, 984.
Jiang, H., Xu, Z., Aluru, M.R., Dong, L., 2014. Plant chip for high-throughput phenotyping of Arabidopsis. Lab Chip 14 (7), 1281–1293.
K'Owino, I.O., Sadik, O.A., 2005. Impedance spectroscopy: a powerful tool for rapid biomolecular screening and cell culture monitoring. Electroanalysis 17 (23), 2101–2113.

Karimi-Maleh, H., Karimi, F., Alizadeh, M., Sanati, A.L., 2019. Electrochemical sensors, a bright future in the fabrication of portable kits in analytical systems. Chem. Rec. 20, 1–12.
Kumar, M., Campbell, L., Turner, S., 2016. Secondary cell walls: biosynthesis and manipulation. J. Exp. Bot. 67 (2), 515–531.
Larkin, P.J., 1976. Purification and viability determinations of plant protoplasts. Planta 128 (3), 213–216.
Le Gall, H., Philippe, F., Domon, J.M., Gillet, F., Pelloux, J., Rayon, C., 2015. Cell wall metabolism in response to abiotic stress. Plants 4 (1), 112–166.
Li, H., Multari, C., Palego, C., Ma, X., Du, X.T., Ning, Y.Q., Buceta, J., Hwang, J.C.M., Cheng, X.H., 2018. Differentiation of live and heat-killed E-coli by microwave impedance spectroscopy. Sensor. Actuator. B Chem. 255, 1614–1622.
Libault, M., Pingault, L., Zogli, P., Schiefelbein, J., 2017. Plant systems biology at the single-cell level. Trends Plant Sci. 22 (11), 949–960.
Liu, H., Tang, X., Lu, H., Xie, W., Hu, Y., Xue, Q., 2020. An interdigitated impedance microsensor for detection of moisture content in engine oil. Nanotechnol. Precis. Eng. https://doi.org/10.1016/j.npe.2020.04.001. https://search.crossref.org/?q=Liu%2C+H.%2C+Tang%2C+X.%2C+Lu%2C+H.%2C+Xie%2C+W.%2C+Hu%2C+Y.%2C+Xue%2C+Q.%2C+2020.+An+interdigitated+impedance+microsensor+for+detection+of+moisture+content+in+engine+oil.+Nanotechnol.+Precis.+Eng.
Malleo, D., Nevill, J.T., Lee, L.P., Morgan, H., 2010. Continuous differential impedance spectroscopy of single cells. Microfluid. Nanofluidics 9 (2–3), 191–198.
Mcdonald, J.C., Whitesides, G.M., 2002. Poly(dimethylsiloxane) as a material for fabrication of microfluidic devices. Acc. Chem. Res. 35 (7), 491–499.
McFarlane, H.E., Doring, A., Persson, S., 2014. The cell biology of cellulose synthesis. Annu. Rev. Plant Biol. 65, 69–94.
McGrath, J.S., Honrado, C., Spencer, D., Horton, B., Bridle, H.L., Morgan, H., 2017. Analysis of parasitic Protozoa at the single-cell level using microfluidic impedance cytometry. Sci. Rep. 7 (1), 2601.
Mockaitis, K., Estelle, M., 2008. Auxin receptors and plant development: a new signaling paradigm. Annu. Rev. Cell Dev. Biol. 24, 55–80.
Morgan, H., Sun, T., Holmes, D., Gawad, S., Green, N.G., 2007. Single cell dielectric spectroscopy. J. Phys. D Appl. Phys. 40 (1), 61–70.
Nagata, T., Takebe, I., 1970. Cell wall regeneration and cell division in isolated tobacco mesophyll protoplasts. Planta 92 (4), 301–308.
Ng, J.M., Gitlin, I., Stroock, A.D., Whitesides, G.M., 2002. Components for integrated poly(dimethylsiloxane) microfluidic systems. Electrophoresis 23 (20), 3461–3473.
Novakovic, L., Guo, T., Bacic, A., Sampathkumar, A., Johnson, K.L., 2018. Hitting the wall-sensing and signaling pathways involved in plant cell wall remodeling in response to abiotic stress. Plants 7 (89), 1–25.
Oikawa, A., Lund, C.H., Sakuragi, Y., Scheller, H.V., 2013. Golgi-localized enzyme complexes for plant cell wall biosynthesis. Trends Plant Sci. 18 (1), 49–58.
Ronkainen, N.J., Halsall, H.B., Heineman, W.R., 2010. Electrochemical biosensors. Chem. Soc. Rev. 39 (5), 1747–1763.
Sakai, K., Charlot, F., Le Saux, T., Bonhomme, S., Nogue, F., Palauqui, J.C., Fattaccioli, J., 2019. Design of a comprehensive microfluidic and microscopic toolbox for the ultra-wide spatio-temporal study of plant protoplasts development and physiology. Plant Methods 15 (79), 1–12.
Sakamoto, S., Somssich, M., Nakata, M.T., Unda, F., Atsuzawa, K., Kaneko, Y., Wang, T., Bagman, A.M., Gaudinier, A., Yoshida, K., Brady, S.M., Mansfield, S.D., Persson, S., Mitsuda, N., 2018. Complete substitution of a secondary cell wall with a primary cell wall in Arabidopsis. Native Plants 4 (10), 777–783.
Samuels, A.L., Giddings Jr., T.H., Staehelin, L.A., 1995. Cytokinesis in tobacco BY-2 and root tip cells: a new model of cell plate formation in higher plants. J. Cell Biol. 130 (6), 1345–1357.
Sanati Nezhad, A., 2014. Microfluidic platforms for plant cells studies. Lab Chip 14 (17), 3262–3274.
Somerville, C., Bauer, S., Brininstool, G., Facette, M., Hamann, T., Milne, J., Osborne, E., Paredez, A., Persson, S., Raab, T., Vorwerk, S., Youngs, H., 2004. Toward a systems approach to understanding plant cell walls. Science 306 (5705), 2206–2211.
Song, H., Wang, Y., Rosano, J.M., Prabhakarpandian, B., Garson, C., Pant, K., Lai, E., 2013. A microfluidic impedance flow cytometer for identification of differentiation state of stem cells. Lab Chip 13 (12), 2300–2310.
Sugimoto, K., Williamson, R.E., Wasteneys, G.O., 2001. Wall architecture in the cellulose-deficient rsw1 mutant of Arabidopsis thaliana: microfibrils but not microtubules lose their transverse alignment before microfibrils become unrecognizable in the mitotic and elongation zones of roots. Protoplasma 215 (1–4), 172–183.
Sun, T., Green, N.G., Morgan, H., 2008. Analytical and numerical modeling methods for impedance analysis of single cells on-chip. Nano 3 (1), 55–63.
Tan, W.H., Takeuchi, S., 2007. A trap-and-release integrated microfluidic system for dynamic microarray applications. Proc. Natl. Acad. Sci. U. S. A. 104 (4), 1146–1151.
Tan, W.H., Takeuchi, S., 2008. Dynamic microarray system with gentle retrieval mechanism for cell-encapsulating hydrogel beads. Lab Chip 8 (2), 259–266.
Teale, W.D., Paponov, I.A., Palme, K., 2006. Auxin in action: signalling, transport and the control of plant growth and development. Nat. Rev. Mol. Cell Biol. 7 (11), 847–859.
Tenhaken, R., 2014. Cell wall remodeling under abiotic stress. Front. Plant Sci. 5 (771), 1–9.
Tran, A.K., Sapkota, A., Wen, J., Li, J., Takei, M., 2018. Linear relationship between cytoplasm resistance and hemoglobin in red blood cell hemolysis by electrical impedance spectroscopy & eight-parameter equivalent circuit. Biosens. Bioelectron. 119, 103–109.
Tsai, S.L., Wang, M.H., 2016. 24 h observation of a single HeLa cell by impedance measurement and numerical modeling. Sensor. Actuator. B Chem. 229, 225–231.
Turner, S., Kumar, M., 2018. Cellulose synthase complex organization and cellulose microfibril structure. Philos. Trans. A Math. Phys. Eng. Sci. 376 (2112), 1–11.
Xu, Y., Xie, X., Duan, Y., Wang, L., Cheng, Z., Cheng, J., 2016. A review of impedance measurements of whole cells. Biosens. Bioelectron. 77, 824–836.
Yoo, S.D., Cho, Y.H., Sheen, J., 2007. Arabidopsis mesophyll protoplasts: a versatile cell system for transient gene expression analysis. Nat. Protoc. 2 (7), 1565–1572.
Zhang, F., Jin, T., Hu, Q., He, P., 2018a. Distinguishing skin cancer cells and normal cells using electrical impedance spectroscopy. J. Electroanal. Chem. 823, 531–536.
Zhang, J., Xie, M., Tuskan, G.A., Muchero, W., Chen, J.G., 2018b. Recent advances in the transcriptional regulation of secondary cell wall biosynthesis in the woody plants. Front. Plant Sci. 9, 1535.
Zheng, Y., Nguyen, J., Wei, Y., Sun, Y., 2013. Recent advances in microfluidic techniques for single-cell biophysical characterization. Lab Chip 13 (13), 2464–2483.
Zhou, Y., Basu, S., Laue, E., Seshia, A.A., 2016. Single cell studies of mouse embryonic stem cell (mESC) differentiation by electrical impedance measurements in a microfluidic device. Biosens. Bioelectron. 81, 249–258.